Critical current density and mechanism of vortex pinning in K_{x}Fe_{2−y}Se_{2} doped with S

Hechang Lei (雷和畅) and C. Petrovic

Critical current density and vortex pinning mechanism of $K_xFe_{2-y}Se_2$ with S doping

Hechang Lei (雷和畅) and C. Petrovic
Condensed Matter Physics and Materials Science Department,
Brookhaven National Laboratory, Upton, NY 11973, USA
(Dated: July 20, 2011)

We report critical current density J_c in $K_xFe_{2-y}Se_{2-z}S_z$ crystals. The J_c can be enhanced significantly with optimal S doping (z = 0.99). For $K_{0.70(7)}Fe_{1.55(7)}Se_{1.01(2)}S_{0.99(2)}$ the weak fishtail effect is found for H∥c. The normalized vortex pinning forces follow the scaling law with maximum position at 0.41 of reduced magnetic field. These results demonstrate that the small size normal point defects dominate the vortex pinning mechanism.

PACS numbers: 74.25.Sv, 74.25.Wx, 74.25.Ha, 74.70.Xa

I. INTRODUCTION

Since the discovery of $LaFeAsO_{1-x}F_x$ (FeAs-1111 type) with $T_c = 26$ K,[1] intensive studies have been carried out in order to understand the superconducting mechanism, explore new materials and possible technical applications. Among discovered iron-based superconductors, FeAs-1111 materials and AFe_2As_2 (A = alkaline or alkaline-earth metals, FeAs-122 type) exhibit high upper critical fields (μ_0H_{c2}) and good current carrying ability which are important for energy applications.[2−5] On the other hand, even though FeCh (Ch = S, Se, and Te, FeCh-11 type) materials have nearly isotropic high μ_0H_{c2} and considerable critical current density,[6,7] their relatively low T_c when compared to FeAs-1111 and FeAs-122 superconductors is a serious disadvantage. Recently, $A_xFe_{2-y}Se_2$ (A = K, Rb, Cs, and Tl, AFeCh-122 type) materials attracted much attention due to rather high $T_{c,onset}$ ($\sim$ 32 K), and μ_0H_{c2}($\sim$ 56 T for H∥c at 1.6 K).[8,9] However, preliminary studies indicate that the critical current density in $K_xFe_{2-y}Se_2$ is lower than in other iron based superconductors.[10,11] Therefore, it is important to explore pathways for the critical current density J_c enhancement in AFeCh-122 compounds.

In present work, we report the enhancement of critical current density and vortex pinning mechanism in $K_xFe_{2-y}Se_{2-z}S_z$ single crystals. Point defect pinning dominates the vortex pinning mechanism whereas critical current density is maximized for z = 0.99(2).

II. EXPERIMENT

Details of crystal growth and structure characterization were reported in previous work.[10,12] Crystals were polished into rectangular bars and magnetization measurements were performed in a Quantum Design Magnetic Property Measurement System (MPMS-XL5) up to 5 T. The average stoichiometry and homogeneity of samples were determined by examination of multiple points using an energy-dispersive x-ray spectroscopy (EDX) in a JEOL JSM-6500 scanning electron microscope.
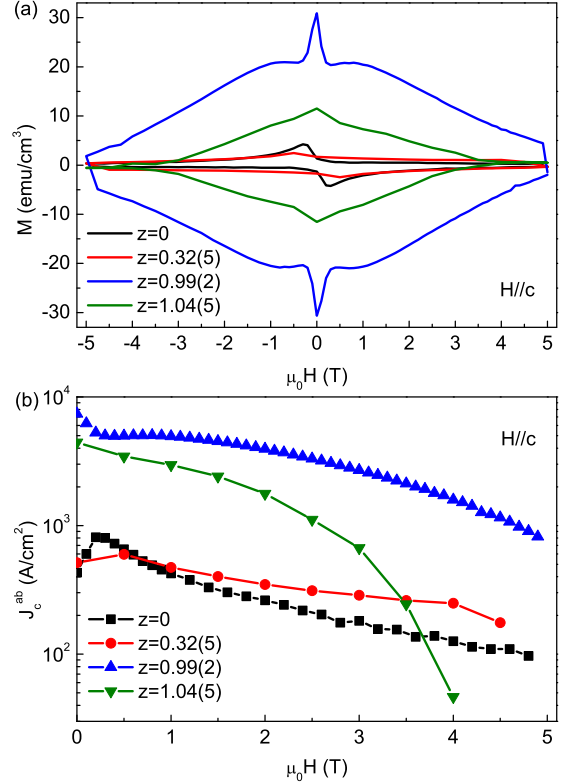

FIG. 1.   (a) Magnetization hysteresis loops of $K_xFe_{2-y}Se_{2-z}S_z$ at 1.8 K for H∥c.   (b) Superconducting critical current densities $J_c^{ab}(\mu_0H)$ determined from magnetization measurements using the Bean model.

III. RESULTS

Fig. 1(a) shows magnetization hysteresis loops (MHLs) of $K_xFe_{2-y}Se_{2-z}S_z$ at 1.8 K for H∥c with field up to 5 T. The shapes of MHLs for all of samples are typical of type-II superconductors. However, for different S doping, they exhibit different flux pinning behavior. For low S doping (z = 0 and z = 0.32), the MHLs are asymmetric. This asymmetry suggests that the bulk pinning is small and that the influence of the surface barrier is important.[13,14] On the other hand, for higher S doping (z = 0.99 and z = 1.04), the shapes of MHLs are
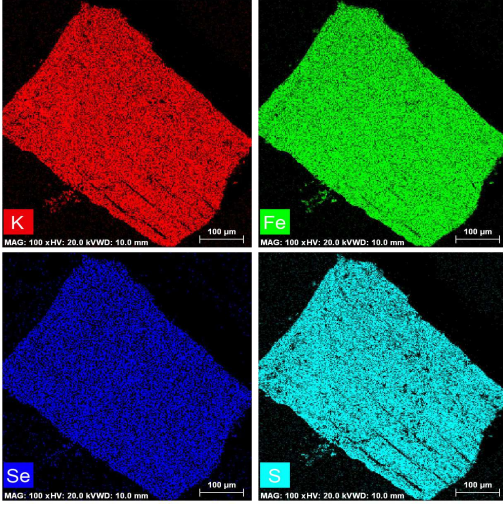
FIG. 2. EDX mapping of $K_{0.70(7)}Fe_{1.55(7)}Se_{1.01(2)}S_{0.99(2)}$. (Scale bar is 0.1 mm.)

symmetric indicating that the bulk pinning is dominant. For $K_{0.70(7)}Fe_{1.55(7)}Se_{1.01(2)}S_{0.99(2)}$ crystal, a small fishtail hump appears at 0.8 T, similarly to FeAs-122 single crystals.[5,15−17] We determine the critical current density from the Bean model.[18,19] For a rectangularly-shaped crystal with dimension c < a < b, when H∥c, the in-plane critical current density $J_c^{ab}(\mu_0 H)$ is given by

$$J_c^{ab}(\mu_0 H) = \frac{20\Delta M(\mu_0 H)}{a(1 - a/3b)} \qquad (1)$$

where a and b (a < b) are the in-plane sample size in cm, $\Delta M(\mu_0 H)$ is the difference between the magnetization values for increasing and decreasing field at a particular applied field value (measured in emu/cm^3), and $J_c^{ab}(\mu_0 H)$ is the critical current density in A/cm^2. From Fig. 1(b), it can be seen that the $J_c^{ab}(\mu_0 H)$ shows small increase at high field region for z = 0.32 when compared to z = 0 sample. On the other hand, it is enhanced about one order of magnitude for z = 0.99 in the whole magnetic field range. For higher S content, the $J_c^{ab}(0)$ is still much larger than in pure $K_{0.64(4)}Fe_{1.44(4)}Se_{2.00(0)}$, but the $J_c^{ab}(\mu_0 H)$ at high fields is smaller. It should be noted that the T_c decreases significantly when z > 0.32. When compared to z = 0 ($T_{c,onset}$ = 33.0 K), z = 0.99 crystal has $T_{c,onset}$ = 24.6 K, whereas z= 1.04 has $T_{c,onset}$ = 18.2 K.[12] Therefore, sample with z = 0.99 exhibits the best performance and we studied its field dependence of magnetization and critical current density in detail. K, Fe, Se and S are uniformly distributed in z = 0.99 crystal (Fig. 2), as is the case with all crystals we investigated.

Fig. 3 shows the MHLs of crystal with z = 0.99 for both field directions. The fishtail effect is only observed for H∥c. It diminishes gradually with increasing temperature. Similar behavior has also been seen in $BaFe_{2-x}Co_x As_2$,[17] suggesting anisotropic flux pinning.[15] On the other hand, linear $M(\mu_0 H)$ background exists
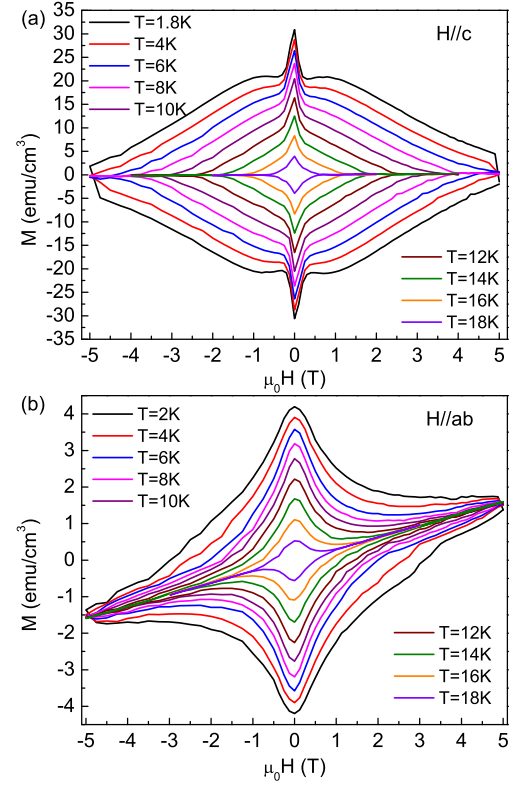

FIG. 3. MHLs of $K_{0.70(7)}Fe_{1.55(7)}Se_{1.01(2)}S_{0.99(2)}$ for (a) H∥c and (b) H∥ab.

for both field directions, being more obvious for H∥ab. This is also observed in pure $K_{0.64(4)}Fe_{1.44(4)}Se_{2.00(0)}$.[10] The slope of this background for crystal with z = 0.99 is nearly the same as in pure material, suggesting that high temperature magnetism changes little with z for z ⩽ 0.99. The linear $M(\mu_0 H)$ background has no effect on the calculation of $\Delta M(\mu_0 H)$, and is due to incomplete superconducting volume fraction of the crystals used in this study. We will discuss the effects of electromagnetic granularity in the next section.

The $J_c^{ab}(\mu_0 H)$ is calculated using eq. (1) for H∥c and shown in Fig. 4(a)The evaluation of critical current density becomes more complex for H∥ab, since there are two different contributions. One is vortex motion across the planes, $J_c^c(\mu_0 H)$, and the other is vortex motion parallel to the planes, $J_c^{\parallel}(\mu_0 H)$. Usually, $J_c^{\parallel}(\mu_0 H) \neq J_c^{ab}(\mu_0 H)$. Assuming $a, b \gg c/3 \cdot J_c^{\parallel}(\mu_0 H)/J_c^c(\mu_0 H)$,[19] we obtain $J_c^c(\mu_0 H) \approx 20\Delta M(\mu_0 H)/c$. The calculated $J_c^c(\mu_0 H)$ is shown in Fig. 3(b).

The $J_c^{ab}(0)$ and $J_c^c(0)$ are 7.4 and 8.4×10^3 A/cm^2 at 1.8 K and 2 K, respectively. Even though they are still smaller than in other iron pnictide superconductors (where critical current densities are usually above 10^5 A/cm^2 at 5 K),[15,20] S doping significantly enhances the critical current density when compared to pure $K_{0.64(4)}Fe_{1.44(4)}Se_{2.00(0)}$.[10,11] It suggests that S doping introduces effective pinning center and therefore enhances the J_c for both field directions. On the
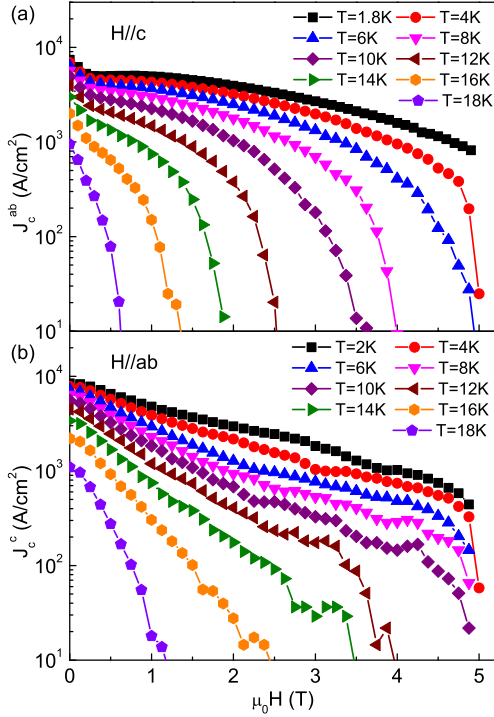
FIG. 4. Magnetic field dependence of superconducting critical current densities (a) $J_c^{ab}(\mu_0 H)$ and (b) $J_c^c(\mu_0 H)$ for $K_{0.70(7)}Fe_{1.55(7)}Se_{1.01(2)}S_{0.99(2)}$.
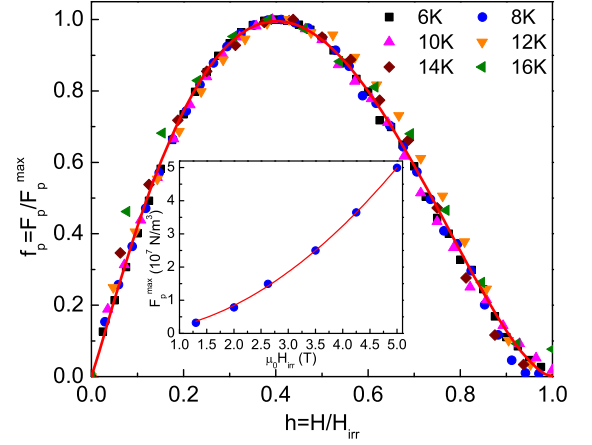

FIG. 5. Normalized flux pinning force $f_p = F_p/F_p^{\max}$ as a function of reduced field $h = H/H_{irr}$ for $K_{0.70(7)}Fe_{1.55(7)}Se_{1.01(2)}S_{0.99(2)}$. Solid line represents the fitting curve using $f_p = Ah^p(1-h)^q$. Inset shows $F_p^{\max}$ as a function of $\mu_0 H_{irr}$. Solid line shows the fitting result obtained by using $F_p^{\max} = A(\mu_0 H_{irr})^\alpha$.

other hand, the ratio of $J_c^c(\mu_0 H)/J_c^{ab}(\mu_0 H)$ is approximately 1 and is smaller than in $BaFe_{2-x}Co_xAs_2$.[20] The field dependence of $J_c^c(\mu_0 H)$ is somewhat weaker than $J_c^{ab}(\mu_0 H)$. This could be related to the layered structure of $K_xFe_{2-y}Se_{2-z}S_z$.

IV. DISCUSSION

In order to gain more insight into the vortex pinning mechanism in $K_{0.70(7)}Fe_{1.55(7)}Se_{1.01(2)}S_{0.99(2)}$, we plot the normalized vortex pinning force $f_p = F_p/F_p^{\max}$ as a function of the reduced field $h = H/H_{irr}$ at various temperatures for H∥c (Fig. 5). The pinning force F_p was obtained from the critical current density using $F_p = \mu_0 H J_c$, and $F_p^{\max}$ corresponds to the maximum pinning force. The irreversibility field $\mu_0 H_{irr}$ is the magnetic field at which $J_c^{ab}(T, \mu_0 H)$ is zero. It can be clearly seen that the f_p vs h curves exhibit scaling behavior, independent of temperature, suggesting dominance of single vortex pinning mechanism. Scaling law $f_p \propto h^p(1-h)^q$ explains well our data.[21] The obtained parameters are $p = 1.10(1)$ and $q = 1.64(2)$. The value of $h_{\max}^{fit} (= p/(p+q)) \approx 0.40$ is consistent with the peak positions ($h_{max}^{exp} \approx 0.41$) of the experimental f_p vs h curves at various temperatures. According to the Dew-Hughes model for pinning mechanism,[21] the $h_{max} = 0.33$ with $p = 1$ and $q = 2$ corresponds to small size normal point defects pinning. Our results indicate that small normal point defects pinning dominates vortex pinning mech-

anism. These defects could be related to distribution of S ions on a submicron scale, similarly to FeAs-122 system.[5,15,16] Moreover, the $F_p^{\max}$ can be fitted using $F_p^{\max} = A(\mu_0 H_{irr})^\alpha$ and we obtain $\alpha = 1.94(3)$. This is consistent with the theoretical value ($\alpha = 2$).[21]

Since our crystals are rather homogeneous (Fig. 2), the shape of M(H) for z = 0 and z = 0.32 suggests some electromagnetic granularity similar to $SmFeAsO_{0.85}F_{0.15}$.[22] Since we used the full sample dimensions in J_c^{ab} and J_c^c calculation, the values we obtained represent the lower limit of bulk superconducting crystals. Indeed, very recently Gao et al. reported the J_c of $K_xFe_{2-y}Se_2$ can be enhanced significantly (about 1.7×10^4 A/cm^2 at 5 K) using one-step technique.[23] It implies that with S doping, the J_c of AFeCh-122 might increase further if preparation process can be optimized.

V. CONCLUSION

In summary, we show an order of magnitude increases in J_c by S doping in $K_xFe_{2-y}Se_2$. The optimum S content in $K_xFe_{2-y}Se_{2-z}S_z$ single crystals is z = 0.99. For the optimally doped sample, the weak fishtail effect is observed when H∥c. The analysis of vortex pinning force indicates that the dominant pinning sources are small size normal point defects which could originate from distribution of doped S. The results demonstrate that by further optimizing the vortex pinning force, higher values of J_c could be achieved, raising the prospects for technical applications of AFeCh-122 compounds.

VI. ACKNOWLEDGEMENTS

[1] Y. Kamihara, T. Watanabe, M. Hirano, and H. Hosono, J. Am. Chem. Soc. **130**, 3296 (2008).

[2] F. Hunte, J. Jaroszynski, A. Gurevich, D. C. Larbalestier, R. Jin, A. S. Sefat, M. A. McGuire, B. C. Sales, D. K. Christen, and D. Mandrus, Nature **453**, 903 (2008).

[3] H. Q. Yuan, J. Singleton, F. F. Balakirev, S. A. Baily, G. F. Chen, J. L. Luo, and N. L. Wang, Nature **457**, 565 (2009).

[4] J. Karpinski, N. D. Zhigadlo, S. Katrych, Z. Bukowski, P. Moll, S. Weyeneth, H. Keller, R. Puzniak, M. Tortello, D. Daghero, R. Gonnelli, I. Maggio-Aprile, Y. Fasano, Ø. Fischer, K. Rogacki, and B. Batlogg, Physica C **469**, 370 (2009).

[5] H. Yang, H. Luo, Z. Wang, and H. H. Wen, Appl. Phys. Lett. **93**, 142506 (2008).

[6] H. C. Lei, R. W. Hu, E. S. Choi, J. B. Warren, and C. Petrovic, Phys. Rev. B **81**, 094518 (2010).

[7] C. S. Yadav and P.L. Paulose, Physica C **151**, 216 (2009).

[8] J. Guo, S. Jin, G. Wang, S. Wang, K. Zhu, T. Zhou, M. He, and X. Chen, Phys. Rev. B **82**, 180520(R) (2010).

[9] E. D. Mun, M. M. Altarawneh, C. H. Mielke, V. S. Zapf, R. Hu, S. L. Bud'ko, and P. C. Canfield, Phys. Rev. B **83**, 100514(R) (2011).

[10] H. C. Lei and C. Petrovic, Phys. Rev. B **83**, 184504 (2011).

[11] R. Hu, K. Cho, H. Kim, H. Hodovanets, W. E. Straszheim, M. A. Tanatar, R. Prozorov, S. L. Bud'ko, P. C. Canfield, Supercond. Sci. Technol. **24**, 065006 (2011).

[12] H. C. Lei, K. F. Wang, J. B. Warren, and C. Petrovic, arXiv:1102.2434 (2011).

[13] M. Pissas, E. Moraitakis, D. Stamopoulos, G. Papavassil-iou, V. Psycharis, and S. Koutandos, J Supercond. Nov. Magn. **14**, 615 (2001).

[14] L. Zhang, Q. Qiao, X.B. Xu, Y. L. Jiao, L. Xiao, S. Y. Ding, and X. L. Wang, Physica C **445-448**, 236 (2006).

[15] D. L. Sun, Y. Liu, and C. T. Lin, Phys. Rev. B **80**, 144515 (2009).

[16] A. Yamamoto, J. Jaroszynski, C. Tarantini, L. Balicas, J. Jiang, A. Gurevich, D. C. Larbalestier, R. Jin, A. S. Sefat, M. A. McGuire, B. C. Sales, D. K. Christen, and D. Mandrus, Appl. Phys. Lett. **94**, 062511 (2008).

[17] R. Prozorov, N. Ni, M. A. Tanatar, V. G. Kogan, R. T. Gordon, C. Martin, E. C. Blomberg, P. Prommapan, J. Q. Yan, S. L. Bud'ko, and P. C. Canfield, Phys. Rev. B **78**, 224506 (2008).

[18] C. P. Bean, Phys. Rev. Lett. **8**, 250 (1962).

[19] E. M. Gyorgy, R. B. van Dover, K. A. Jackson, L. F. Schneemeyer, and J. V. Waszczak, Appl. Phys. Lett. **55**, 283 (1989).

[20] M. A. Tanatar, N. Ni, C. Martin, R. T. Gordon, H. Kim, V. G. Kogan, G. D. Samolyuk, S. L. Bud'ko, P. C. Canfield, and R. Prozorov, Phys. Rev. B **79**, 094507 (2009).

[21] D. Dew-Hughes, Philos. Mag. **30**, 293 (1974).

[22] C. Senatore, R. Flükiger, M. Cantoni, G. Wu, R. H. Liu, and X. H. Chen, Phys. Rev. B **78**, 054514 (2008).

[23] Z. S. Gao, Y. P. Qi, L. Wang, C. Yao, D. L. Wang, X. P. Zhang, Y. W. Ma, arXiv:1103.2904 (2011).